Bioorganic & Medicinal Chemistry 17 (2009) 2009–2016

Contents lists available at ScienceDirect

Bioorganic & Medicinal Chemistry

journal homepage: www.elsevier.com/locate/bmc

Photodynamic effects of novel 5,15-diaryl-tetrapyrrole derivatives on human colon carcinoma cells

Marzia B. Gariboldi [a], Raffaella Ravizza [a], Peter Baranyai [b], Enrico Caruso [a], Stefano Banfi [a,*], Stefania Meschini [c], Elena Monti [a]

[a] DBSF—Section of Pharmacology, University of Insubria, Via A. da Giussano 10, 21052 Busto Arsizio (VA), Italy
[b] Chemical Research Center, Hungarian Academy of Sciences, PO Box 17, H-1525 Budapest, Hungary
[c] Department of Technology and Health, Italian National Institute of Health, Viale Regina Elena 299, 00161 Rome, Italy

ARTICLE INFO

Article history:
Received 21 October 2008
Revised 7 January 2009
Accepted 10 January 2009
Available online 22 January 2009

Keywords:
Photodynamic therapy
Apoptosis
Reactive oxygen species (ROS)
Nitric oxide
Diarylporphyrins
Diarylchlorin

ABSTRACT

Preliminary in vitro cytotoxicity studies on a panel of *meso* diaryl-substituted tetrapyrrole derivatives newly synthesized in our laboratory have shown that these compounds are photodynamically active on the human colon carcinoma cell line HCT116. In the present study, we investigate some mechanistic aspects of the photodynamic action of the most active compounds in the series, namely the 5-phenyl-15-(3-methoxyphenyl)porphyrin (**1**), the 5-phenyl-15-(3-hydroxyphenyl)porphyrin (**2**) and the 5,15-diphenylporphyrin (**3**). The results of the cytotoxicity studies indicate that the novel photosensitisers (PSs) are more potent in vitro than *m*-THPC (Foscan®), a powerful PS already approved for clinical use in photodynamic therapy (PDT). A series of experiments were performed to elucidate a number of aspects in the mechanism of PS-induced phototoxicity, including, intracellular accumulation and subcellular localization of the PSs, induction of apoptosis, and generation of reactive oxygen species (ROS) and NO·. All the compounds tested exhibit similar singlet oxygen quantum yields; differential intracellular accumulation can contribute to the observed differences in phototoxicity. Flow cytometric studies indicate that all the tested compounds induce apoptosis; however, their cytotoxic effect does not seem to rely solely on this process. Generation of significant amounts of reactive oxygen species (ROS) and NO· were also observed; however, the contribution of this latter effect to the overall phototoxicity is unclear. Taken together, our observations suggest that the diaryl derivatives included in the present study could represent promising leads for the development of novel photosensitizing agents.

1. Introduction

Photodynamic therapy (PDT) is a minimally invasive treatment for both neoplastic and non-neoplastic proliferating cell diseases.[1,2] PDT relies on the uptake of a photosensitizing compound by the pathologic tissue. Subsequent activation of the PS by local irradiation with visible light results in singlet oxygen production, which is followed by localized cellular damage. Tumor ablation is thought to depend both on direct lethal effects of PDT on tumor cells and on microvascular injury induced by the treatment, thus limiting tumor blood supply.[2–4] Cell death was initially thought to occur by necrosis; however, apoptosis and, more recently, autophagy have also been implicated in the process, depending on the PS used and its concentration, light dose, oxygen availability and the cell type(s) involved.[5–9]

The first PS to be granted regulatory approval (in 1993) was porfimer sodium (Photofrin®, Axcan Pharma, Montreal, Canada), a mixture of porphyrin oligomers produced by partial purification of hematoporphyrin derivative. Photofrin®-based PDT has proven effective against a variety of tumors, including cancers of the lung, stomach, cervix, bladder and esophagus. However, its weak absorption in the red region of the spectrum ($\geqslant$600 nm, necessary for the PS activation in the deeper tissues with a penetrating red light) and the extended skin photosensitivity make this PS less than ideal for clinical use, thus prompting an active search for novel PSs featuring more favorable properties.[10] Various classes of PSs are currently in clinical use or at different stages of preclinical and clinical development, many of which include the cyclic tetrapyrrole core structure typical of porphyrins (for a recent review see[11]). Among these 'second generation' PSs, the synthetic chlorin derivative 5,10,15,20-tetra(3-hydroxyphenyl)chlorin (*m*-THPC, also known as temoporfin; marketed as Foscan® by Biolitec Pharma, Scotland, UK) is perhaps the most successful, having recently been granted European approval for palliative treatment of patients with advanced head and neck cancers.[12,13] Encouraging preclinical in vitro and in vivo

* Corresponding author. Address: DBSF—University of Insubria, Via H.J. Dunant 3, 21100 Varese (VA), Italy. Tel.: +39 0332 421550; fax: +39 0332 421554.
E-mail address: stefano.banfi@uninsubria.it (S. Banfi).

0968-0896/$ - see front matter © 2009 Elsevier Ltd. All rights reserved.
doi:10.1016/j.bmc.2009.01.035

results have been reported by Patrice and co-workers,[14] using a diaryl-substituted porphyrin derivative. More recently, our group has synthesized a series of novel 5,15-diaryl-tetrapyrrole derivatives, most of which show greater phototoxicity than either Photofrin® or *m*-THPC in a human colon cancer cell line in a preliminary in vitro screening.[15]

In the present study, we focus on the most active compounds from this preliminary screen (Fig. 1), and we assess some mechanistic aspects of their photodynamic activity in the human colon carcinoma cell line HCT116. Thus, a series of experiments have been performed in vitro with photosensitizers **1**, **2**, and **3,** using *m*-THPC as reference compound and a 500 W tungsten–halogen white lamp to irradiate the cells. Besides the dose–response curves, the effects of the PSs on the following issues were investigated: (a) intracellular generation of oxidizing species, including singlet oxygen as well as other reactive oxygen species (ROS) and with a special emphasis on NO·; (b) intracellular accumulation and subcellular distribution of the PSs; (c) involvement of apoptosis in PS-induced cell death; (d) cell cycle distribution; (e) expression of a small panel of proteins involved in apoptosis control. The results reported here confirm what we have recently published[15], namely that the novel diaryl-substituted porphyrins are generally more active, at least in vitro, than *m*-THPC. These observations suggest that porphyrins in this class are promising candidates for further transformation into the corresponding chlorin derivatives, yielding potent PSs suitable for in vivo photodynamic therapy. This is confirmed by the superior phototoxicity exhibited by the chlorin derivative obtained from compound **2** as compared with *m*-THCP.

2. Results

2.1. Phototoxicity studies and Western blot analysis

Table 1 reports the IC_{50} values extrapolated from the dose–response curves obtained with HCT116 cells following PDT with the four PSs (Fig. 1), irradiating with white light. Intrinsic cytotoxicity of the PSs, assessed by omitting the irradiation step from the treatment protocol, was found to be negligible in all cases, up to PS concentrations 10-fold higher than those used for PDT experiments (not shown). Overall, the newly synthesized derivatives were more phototoxic than *m*-THPC, even though statistically significant differences in potency were only achieved by compound **2,** versus both *m*-THPC and the other two diaryl derivatives **1** and **3**.

Table 1
IC_{50} values obtained with HCT116 cells following 24 h exposure to the PSs, 2 h irradiation in PS-free PBS and 24 h incubation in PS-free complete medium

	IC_{50} (nM)
m-THPC	7.6 ± 0.57
1	5.94 ± 0.85
2	1.06 ± 0.15*
3	5.66 ± 1.16

Mean ± SE of 3–4 independent experiments.
* $p < 0.05$ versus all other PSs.

Figure 2A shows apoptosis induction following 24 h exposure to equitoxic concentrations (IC_{50}) of the PSs, followed by 2 h irradiation and 24 h incubation in PS-free medium. All the PSs tested were able to induce apoptosis to some extent, even though the increase in apoptotic cells over control samples only attained statistical significance in the case of *m*-THPC; no significant differences could be observed among all treated groups. Western blot analysis of total protein extracts from treated cells indicates a decrease in the expression of antiapoptotic proteins, such as Bcl2 and survivin, and an increase in the proapoptotic factor Bax, as compared to control cells (Fig. 2B). Such alterations are more marked in extracts from *m*-THPC-treated cells, supporting the stronger proapoptotic activity exhibited by this compound. Cell cycle analysis did not show any significant modifications in cell distribution (Table 2); more specifically, treated cells do not appear to arrest in the G1 or G2/M phases of the cell cycle.

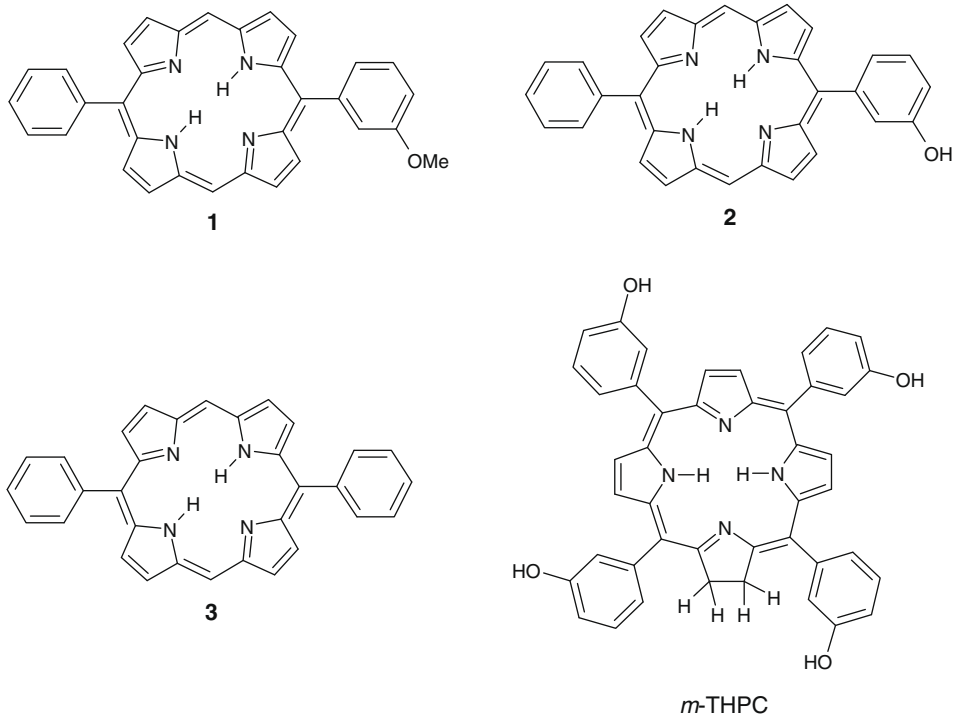

Figure 1. Chemical structures of the 5,15-diarylporphyrins (**1**–**3**) and of *m*-THPC.

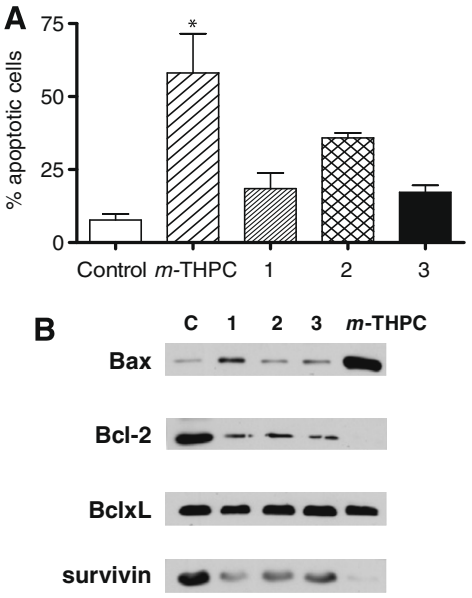

Figure 2. Panel A: Induction of apoptosis in HCT116 cells following 24 h exposure to the PSs at their respective IC_{50} values, 2 h irradiation in PS-free PBS and 24 h incubation in PS-free complete medium. The percentage of apoptotic cells was determined by flow cytometry. Mean ± SE of 3 independent experiments. $^{*}p < 0.05$ versus control. Panel B: Bax, Bcl2, $Bclx_L$, and survivin protein levels in HCT116 cells under the same experimental conditions as in panel A.

Table 2
Cell cycle distribution of HCT116 cells following 24 h exposure to the PSs, 2 h irradiation in PS-free PBS and 24 h incubation in PS-free complete medium

	G1	S	G2/M
Control	53.67 ± 2.46	16.42 ± 0.7	29.90 ± 1.847
m-THPC	51.53 ± 2.62	21.29 ± 0.97	27.17 ± 2.23
1	52.40 ± 0.13	17.93 ± 1.013	29.60 ± 0.9
2	49.03 ± 1.98	21.28 ± 2.03	29.69 ± 0.97
3	52.83 ± 0.76	17.89 ± 1.32	29.27 ± 1.875

Mean ± SE of 3 independent experiments.

2.2. Intracellular PS accumulation and singlet oxygen quantum yield

Following 24 h incubation in the presence of 1 μg/ml of the compounds tested (**1**–**3** and *m*-THPC), very different intracellular amounts of the compounds could be detected by UV spectrophotometry, with the three diaryl compounds accumulating to significantly greater extents than *m*-THPC (Fig. 3). No significant differences were observed in the singlet oxygen quantum yields (Φ_Δ) obtained for compounds **1**–**3** (0.83, 0.84, and 0.91 for **1**, **2**, and **3,** respectively); these values were also comparable to that obtained for *m*-THPC (0.88).

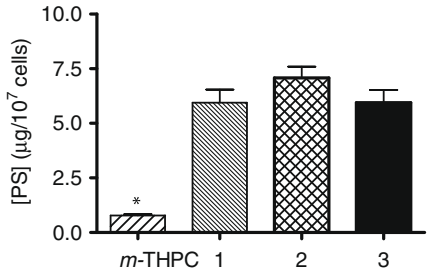

Figure 3. Intracellular PS accumulation in HCT116 cells following 24 h exposure to the different PSs (1 μg/ml), as assessed on cell lysates by UV–Vis spectroscopy in the 400–750 nm wavelength range. The experiment was repeated twice with comparable results. $^{*}p < 0.05$ versus all other PSs.

2.3. Subcellular localization

Figure 4 shows the images obtained by LSCM on HCT116 cells treated with *m*-THPC and compound **2** and incubated with MitoTracker or LysoTracker Green; the images have been obtained by merging the fluorescence of the probes (green) with that of the PSs (red). *m*-THPC localizes both to the mitochondria and the lysosomes (Fig. 4A and B), whereas compound **2** substantially exhibits a lysosomal localization (Fig. 4C and D). Moreover, compound **2**-related fluorescence displays a punctate distribution in the cytoplasm that does not overlap with that of either probe, indicating possible additional localization in other organelles.

2.4. Intracellular oxidizing species

Figure 5 shows the levels of intracellular oxidizing species in PS-treated cells. At the end of the 2 h irradiation period, equitoxic concentrations of the PSs induced variable increases in ROS generation over control levels, even though statistical significance was only attained for compound **2**; in addition, compound **2** was found to be significantly more effective than all the other PSs in generating oxidizing species (Fig. 5A). This trend was maintained when ROS levels were determined 24 h later (data not shown); at that time the absolute intensities of dichlorofluorescein (DCF) fluorescence had decreased, but were still clearly detectable, suggesting that ROS generation may continue for some time after the end of the irradiation.

2.5. $NO^{\cdot}$ generation

The generation of $NO^{\cdot}$ by PSs was determined based on nitrite accumulation in culture supernatants. At the end of the irradiation, low nitrite concentrations were detected in the supernatants, with non-significant differences among different PSs (not shown); however, nitrites accumulated over the following 24 h in PS-free medium, at the end of which significant differences between treatments and control, as well as among treatments, were observed (Fig. 5B). A significant correlation was established between the PS concentrations corresponding to the IC_{50} and the amounts of nitrites released in the culture medium ($r = -0{,}9584$; $p < 0.05$). Inhibition of $NO^{\cdot}$ generation by simultaneous incubation with compound **2** and the $NO^{\cdot}$-synthase (NOS) inhibitor L-NMMA (1 mM) did not significantly modify the photodynamic effect of the PS, yielding an IC_{50} value of 0.683 ± 0.083 ng/ml for compound **2** alone versus 0.482 ± 0.152 ng/ml in the presence of L-NMMA (mean ± SD of 3 independent experiments).

2.6. Synthesis and evaluation of photodynamic activity of chlorin 4

Compound **4** (Fig. 6) was synthesized in 60% yield via diimide reduction of the parental porphyrin **2**.[15] The phototoxic efficacy of Chlorin **4** was assessed as described in Section 2.1, although a LED red light (maximum emission at 635 nm) has been used in these experiments instead of the tungsten–halogen 500 W white lamp. The phototoxic effect on HCT116 cells of compound **4** was compared with that of *m*-THPC and of the parent porphyrin and the obtained IC_{50} values were: 1.32 ± 0.16 nM* for compound **4**; 40.95 ± 0.45 nM for *m*-THPC and 3.96 ± 0.28 nM* for compound **2** (mean ± SE of 3 independent experiments, $^{*}p < 0.001$ vs *m*-THPC).

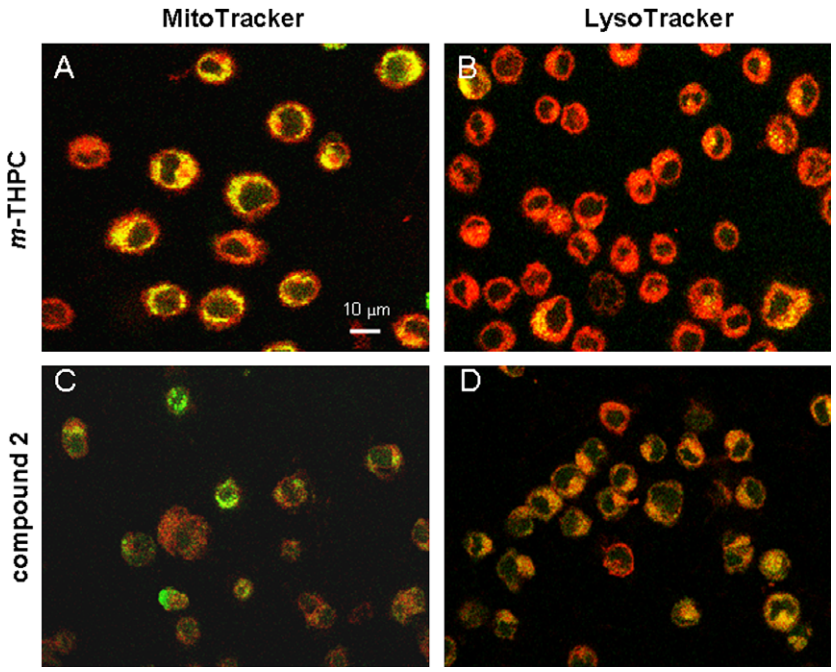

Figure 4. Subcellular localization of *m*-THPC and compound **2**. HCT116 cells were treated for 24 h with *m*-THPC (A and B) or with compound **2** (C and D), both at 500 ng/mL and incubated with MitoTracker Green (A and C) o LysoTracker Green (B and D) before observation with a Leica TCS SP2 spectral confocal microscope (bar = 10 μm).

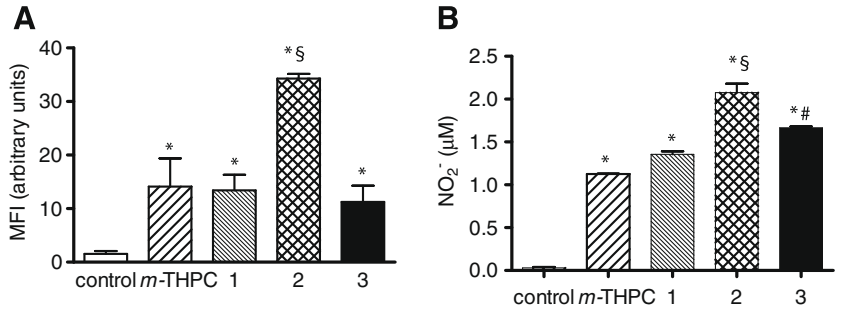

Figure 5. ROS and NO· generation in HCT116 cells following 24 h exposure to the PSs at their respective IC_{50} values and 2 h irradiation in PS-free PBS. (A) The levels of intracellular oxidizing species were determined by flow cytometry at the end of the irradiation period. (B) Nitrite concentration in cell supernatants 24 h after the end of irradiation. The reported values are the mean ± SE of 3 independent experiments. $^{*}p < 0.05$ versus control; $^{\S}p < 0.05$ versus all other PSs; $^{\#}p < 0.05$ versus *m*-THPC and compound **1**.

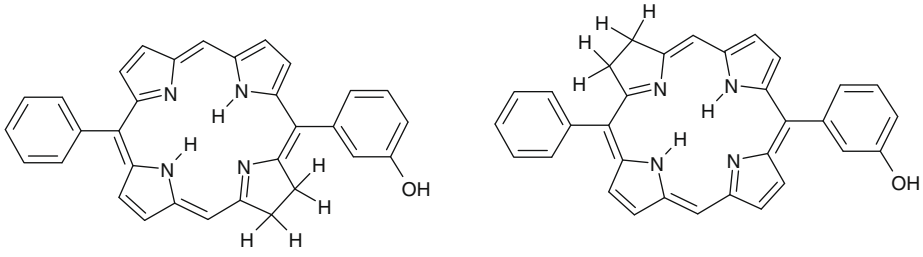

4

mixture of isomers

Figure 6. Chemical structure of the chlorin **4** (two possible isomers).

3. Discussion

The present study investigates some biochemical and biophysical aspects of the in vitro photodynamic effects in human colon cancer cells of three recently described diarylporphyrin PSs. The three PSs (Fig. 1) were selected from a panel of 13 previously synthesized analogs, due to their superior photodynamic activity in HCT116 cells: in this cell line their effects compared favorably with those of already approved compounds for clinical use, namely Photofrin® and *m*-THPC.[15] The results of the present study corrob-

orate our previous findings and provide some insights into the mechanism of action of these compounds.

Regarding the type of cell death induced by the three diarylporphyrin derivatives in HCT116 cells, our results indicate that it occurs at least in part through apoptosis, similarly to what has been described for *m*-THPC[5,16] (Fig. 2A); the stronger proapoptotic effect observed for *m*-THCP is supported by lower levels of the antiapoptotic proteins Bcl-2 and survivin and higher levels of the proapoptotic protein Bax (Fig. 2B). However, it should be noted that other modalities of cell death have been reported following PDT, including necrosis and autophagic cell death;[9,17] the present study does not specifically address this issue, and therefore we cannot rule out that either or both may significantly contribute to the overall cytotoxicity.

Subcellular localization has been reported to dictate the primary cell damage following PDT and the subsequent activation of cell death programs.[18–20] Therefore, an assessment of subcellular localization has been performed by LSCM on cells incubated with *m*-THPC and compound **2**, the most active PS tested, using a PS concentration of 500 ng/ml for 24 h and the organelle-specific fluorescent probes MitoTracker Green and LysoTracker Green. Interestingly, we observed that *m*-THPC co-localizes with both fluorescent probes (which indicates both a mitochondrial and a lysosomal localization) (Fig. 4A and B), whereas compound **2**-related fluorescence exhibits a punctate distribution pattern that only partially overlaps with that of LysoTracker (Fig. 4B and C).

The different localization of the two compounds could explain, at least in part, the observed difference in apoptosis induction, since PSs localized in the mitochondria seem to be more efficient in activating the intrinsic apoptotic pathway.[3] However, as discussed below, the ability to induce photodynamic cell kill does not seem to rely on apoptosis induction alone. Interestingly, the observation that LysoTracker and compound **2**-related fluorescence emissions only partially overlap indicates that other organelles, such as the endoplasmic reticulum (ER) or Golgi apparatus, may be a site of localization for this PS. Indeed, the role of ER in PDT-induced cell death has recently been the object of extensive revision.[17,18] Further investigations will be required in order to elucidate the role played by this organelle in the phototoxic damage induced by compound **2**.

The lack of significant differences in apoptosis induction following exposure to equitoxic concentrations of the three diarylporphyrin derivatives (corresponding to their respective IC_{50} values) indicates that, provided that sufficient intracellular concentrations are achieved, all of them are able to trigger apoptosis, which tends to rule out the hypothesis that the diarylporphyrins tested may differ from one another due to their intrinsic proapoptotic properties. Thus, the ability to achieve effective intracellular levels could be a determinant of the observed differences in potency. Indeed, we have observed that the three diaryl derivatives, which overall are more potent than *m*-THPC, are also accumulated to a greater extent after 24 h (Fig. 3); however, the observation that the three diaryl derivatives exhibit significant differences in phototoxicity, despite their being accumulated to similar extents, suggests that other factors may be involved.

We then focused on the ability of the PSs to generate oxidizing species. It is generally acknowledged that ROS generation is crucial to the successful application of PDT, and both type I and type II photodynamic reactions have been implicated in tumor cell response to this treatment.[21–23] Regarding type II mechanism, measurements of singlet oxygen quantum yields did not help explain the different potencies of the four PSs, as similar high values were found for all three diarylporphyrins, which were also comparable to the value obtained for the less effective *m*-THPC. Next, we proceeded to assess the overall ROS production by equitoxic concentrations of the PSs (corresponding to their respective IC_{50} values). Flow cytometric analysis of DCF fluorescence at end of 2 h irradiation indicated that compound **2** is significantly more active as a ROS generator than all the other compounds tested, and even 24 h later significantly higher ROS levels were detected in cells treated with this PS; in contrast, no significant differences could be observed between the two other diaryl derivatives and *m*-THPC.

Based on the observations reported above, it can be hypothesized that compound **2** relies more heavily on ROS production to achieve its phototoxic effect than the other compounds. However, it should be noted that DCF is a rather non-selective probe for oxidizing species and that it has been shown to react with a number of oxidant species, including NO·, a gaseous free radical that mediates a variety of physiological functions and pathological processes[24], and particularly peroxynitrite ($ONOO^-$), a powerful oxidant resulting from the reaction of NO· with superoxide anion.[25] This last observation is particularly interesting, as generation of NO· has been demonstrated in PDT-treated tumor cells.[26]

The impact of NO· generation on the outcome of PDT is debated: a number of reports indicate that NO· is a key mediator of PDT-induced cell death,[26–28] whereas other Authors have highlighted a cytoprotective role of NO· during PDT.[29–32] In the present study, NO· generation was indeed associated with photosensitization by the compounds tested: at the IC_{50}, the amount of nitrites recovered in cell supernatants was in excellent agreement with the PS concentration, that is, the extent of NO· generation was related to the amount of PS (presumably) present within the cells, but not to the overall photodynamic activity, as indicated by the fact that half-maximal cell kill was associated with the presence of widely different amounts of released nitrites. This observation, together with the failure of the NOS-inhibitor L-NMMA to significantly inhibit or enhance the potency of compound **2**, questions the hypothesis of a causal role of NO· in PS-induced cell damage. NO· generation during PDT seems to be a mere coincidental, concentration-dependent cellular response, possibly representing a defense mechanism, that is however unable to overthrow the final outcome of PDT treatment.

Based on the results of the present study, we can conclude that the photodynamic effects of the three diarylporphyrin PSs compare favorably with those of *m*-THPC, which may warrant in vivo testing, most notably as regards compound **2**. The results obtained within this investigation about some outcomes of the phototoxicity of diarylporphyrins can be summarized in the Table 3, where all data are tentatively reported for each tested photosensitizers in an arbitrary scale.

However, porphyrin-based PSs are less than ideal for in vivo applications, since they are maximally activated by wavelengths in the blue-green region (between 420 and 510 nm) that do not

Table 3
Comparison of the physico-chemical and biological effects of the investigated PSs

	Compound **1**	Compound **2**	Compound **3**	*m*-THPC
IC_{50}	+	+++	+	+
Apoptosis	+	+	+	++
Proapoptotic protein levels	+	+	+	++
Antiapoptotic protein levels	+	+	+	-
Intracellular accumulation	++	++	++	+
Intracellular distribution	Undefined distribution	Lysosomal/other organelles (*not* mitochondrial)	Undefined distribution	Mitochondria/ lysosomal
$^1O_2$	+++	+++	+++	+++
NO·	+	+++	+	+
ROS	+	+++	+	+

achieve a very deep tissue penetration, whereas chlorin-based compounds are photoactivated by wavelengths of ~630–650 nm, reaching deeper into the tumors. Cytotoxicity data obtained with compound 4 seem to justify our expectation that the photodynamic properties of diarylporphyrins are not lost upon conversion to the corresponding chlorins, and indicate this last compound as potential candidates for further development and subsequent in vivo application.

4. Materials and methods

4.1. Photosensitizers and reagents

Compounds **1** [5-phenyl-15-(3-methoxyphenyl)porphyrin], **2** [5-phenyl-15-(3-hydroxyphenyl)porphyrin], and **3** (5,15-diphenylporphyrin) were synthesized by our group as detailed elsewhere.[15] The 5-phenyl-15-(3-hydroxyphenyl)chlorin (**4**) was synthesized from the corresponding porphyrin using the *p*-toluenesulfonylhydrazide ($TsNHNH_2$)/base method. Thus, a $CHCl_3$/MeOH: 9/1 solution of 45 mg (9.41×10^{-2} mmol) of porphyrin **2** was treated with $TsNHNH_2$ (1.94 g, 10.45 mmol) and K_2CO_3 (2.3 g, 16.72 mmol) under reflux for 3 h. After this period the reaction mixture was filtered on Celite and purified by column chromatography (SiO_2, CH_2Cl_2/MeOH: 9/1). A single product was recovered although two possible isomers could be obtained. The desired chlorin was isolated in 59.6% yield (27 mg, 5.7×10^{-2} mmol) as a violet solid. MS-ESI$^+$: *m*/*z* 481.6 [M+1]. Anal. Calcd for $C_{32}H_{24}N_4O$: C, 79.98; H, 5.03; O, 3.33. Found: C, 80.81; H, 5.13; O, 3.29. UV–vis (MeOH): λ_{max}, nm ($\log \varepsilon$) 404 nm (4.64); 508 (3.81); 642 nm (4.01). ^{1}H NMR ($CDCl_3$): −1.91 (s, 1H); −1.45 (s, 1H); 4.39 (dd, 2H); 4.69 (dd, 2H); 7.33 (dd, 1H); 7.52 (t, 1H); 7.66 (dt, 1H); 7.78 (t, 1H); 7.87 (m, 3H); 8.05 (m, 2H); 8.44 (dd, 1H); 8.68 (d, 1H); 8.81 (d, 1H); 8.87 (d, 1H); 8.97 (d, 1H); 9.03 (s, 1H); 9.11 (d, 1H); 9.86 (s, 1H).

m-THPC was kindly provided by Biolitec Pharma, Scotland UK. Stock solutions (1 mg/ml) were prepared in DMSO and diluted in culture medium as required; the final DMSO concentration never exceeded 1%, which was not toxic to HCT116 cell under the drug exposure conditions used in this study. All standard chemicals and cell culture reagents, unless otherwise indicated, were purchased from Sigma–Aldrich s.r.l. (Milan, Italy).

4.2. Cell lines and culture conditions

Human adenocarcinoma HCT116 cells were obtained from the American Type Culture Collection (Rockville, MD, USA) and maintained in DMEM (Dulbecco's Modified Eagle Medium) supplemented with 10% fetal bovine serum (Mascia Brunelli) at 37 °C in a humidified 5% CO_2 atmosphere.

4.3. Phototoxicity studies

Photodynamic cell kill by the different PSs, including *m*-THPC, was assessed on colon cancer cells by a standard colorimetric assay based on the mitochondrial reduction of 3-(4,5-dimethylthiazol-yl)-2,5-diphenyltetrazolium bromide (MTT).[33] Briefly, 1.5×10^4 cells/ml were seeded onto 96-well plates and allowed to grow for 48 h prior to treatment with different PS concentrations. Following 24 h exposure, the PS-containing medium was replaced by phosphate-buffered saline (PBS), in order to avoid interference by phenol red-containing culture medium, and cells were irradiated for 2 h with white light (fluence rate of 20 mW cm^{-2}); to avoid overheating of the cultures during irradiation, a 2 cm thick filter containing recirculating water at rt was interposed between the lamp and the culture plates. To compare the efficacy of [5-phenyl-15-(3-hydroxyphenyl)chlorin] with that of *m*-THPC a light emitting diode (LED) lamp, made by 12 red 1 W lights (maximum fluence rate 0.6 mW cm^{-2} at 630 nm, band width +/− 25 nm, maximum fluence 2.8 J cm^{-2} nm^{-1}) was used as an alternative to the white light for chlorin photo-excitation. At the end of the irradiation, PBS was replaced by drug-free complete medium and the cells were incubated for an additional 24 h period, at the end of which MTT (2 mg/ml in PBS, final concentration 0.4 mg/ml) were added to each well for 3 h at 37 °C. Formazan crystals formed via MTT reduction by metabolically active cells were dissolved in DMSO and the corresponding optical densities were measured at 570 nm using a Universal Microplate Reader EL800 (Bio-Tek Instruments). IC_{50} values were estimated from the resulting concentration–response curves using GraphPad Prism software, v. 4.03. (GraphPad, San Diego, CA, USA). Possible intrinsic (i.e., non-photodynamic) cytotoxic effects of the PS were assessed on cells processed as described above, omitting the irradiation step and using PS concentrations up to 10-fold higher than those used in phototoxicity studies.

4.4. Intracellular PS accumulation

Evaluation of intracellular PS accumulation was performed on HCT116 cells exposed to the four agents (**1**–**3** and *m*-THPC) (1 μg/ml for 24 h); for this set of experiments cells were not irradiated. At the end of the exposure time, treated cells were detached by trypsinization, thoroughly washed in ice-cold PBS and resuspended at 10^7 cells/ml in lysis buffer (1% SDS in 0.1 N NaOH). Intracellular PS accumulation was assessed by UV–Vis spectroscopy on cell lysates diluted with PBS (1:1 v/v); spectra were recorded in the 400–750 nm wavelength range. For each PS, intracellular levels were assessed at the wavelength corresponding to the highest peak absorbance value. Calibration curves were obtained by adding increasing amounts (4–20 μl) of 1 mg/ml DMSO stock solution of the PSs in lysates from untreated cells, diluted in PBS (1:1 v/v) yielding a PS concentration range between 4 and 20 μM.

4.5. Laser scanning confocal microscopy (LSCM)

The subcellular distribution of *m*-THPC and compound **2** was assessed in HCT116 cells following 24 h incubation with the two agents (500 ng/ml), followed by 1 h incubation at 37 °C with the fluorescent probes MitoTracker Green or LysoTracker Green (InVitrogen Molecular Probes), both diluted 1:1000 in culture medium; again, the irradiation step was omitted from the treatment protocol in this set of experiments. The cells were then detached as described above, thoroughly washed and transferred by cytospin (2.5×10^5/sample, 700 rpm for 6 min) onto microscope slides, fixed with 4% paraformaldehyde for 30 min, and examined using a Leica TCS SP2 spectral confocal microscope equipped with Argon–HeliumNeon (Ar–HeNe) laser. Mitochondria- and lysosome-specific probes and PSs were excited at the wavelength of 488 nm; emission lines were collected after passage through a double dichroic (DD488/543) filter in a spectral window ranging from 490 nm to 516 nm for MitoTracker Green and LysoTracker Green, and from 630 nm to 745 nm for the PSs. Signals from the different fluorescent probes were acquired in sequential scan mode, which allows the elimination of channel cross-talk, and co-localization was detected in an overlay mode. Acquisition parameters were as follows: 63.0/1.4 NA objective; image size 1024×1024; pinhole size: 1 Airy; step size: 0.5 μm. Images were processed by using LCS (Leica Microsystems. Heidelberg Gmbh, Germany) and Photoshop (Adobe System Inc. Mountain View, CA, USA) software programs.

4.6. Singlet oxygen quantum yield

Singlet oxygen quantum yields (Φ_Δ) of the PSs **1**–**3** and *m*-THPC were assessed based on singlet oxygen emission at 1.27 μm following laser excitation at 532 nm. The emission decay was monitored by a liquid nitrogen-cooled germanium photodiode (EO-817P, North Coast Scientific Co.). The excitation source was a frequency-doubled Nd:YAG laser (Continuum, Surelite I-10, 4–6 ns pulses at 532 nm). Pulse energy was measured by an energy meter (Rj 7100, Laser Precision Corporation). Two interference filters (centered at 1270 nm, FWHM 40 nm) were placed between the sample and the detector. Solutions of the reference (Rose Bengal sensitizer (Fluka) in ethanol, $\Phi_\Delta = 0.80$, or *meso*-tetraphenylporphyrin (H_2-TPP) in chloroform, $\Phi_\Delta = 0.66$) and tested PSs were prepared in order to obtain similar absorbance values (between 0.30 and 0.67) at 532 nm; for the tested compounds, the concentrations required ranged between 10^{-5} and 10^{-4} M. Measurements were carried out at room temperature (298 K) in chloroform (spectroscopic grade).[34]

4.7. Western blot

Cells were exposed to the different PS at their respective IC_{50} values for 24 h, irradiated in PBS for 2 h, incubated in drug-free medium for 24 h and protein extracts were obtained. In most cases 30 μg of protein per lane were loaded onto polyacrylamide gels (11%) and separated under denaturing conditions; in the case of Bcl2 immunodetection, 150 μg of protein were loaded. Protein bands were then transferred onto Immobilon P membranes (Millipore, Bedford, MA, USA), and Western blot analysis was performed by standard techniques with the following antibodies: mouse monoclonal anti-human Bcl2 (100); rabbit polyclonal anti-human Bax (N-20) (Santa Cruz Biotechnology, Inc., Santa Cruz, CA, USA); mouse monoclonal anti-Bcl-x_L (MBL Co., Japan); rabbit polyclonal anti-survivin (Abcam, Cambridge, UK). Equal loading of the samples was verified by re-probing the blots with a mouse monoclonal anti-actin antibody (Santa Cruz Biotechnology, Inc). Protein bands were visualized using a peroxidase-conjugated anti-mouse/rabbit secondary antibody and the Supersignal West Pico Chemiluminescence Substrate (Pierce, Milan).

4.8. Flow cytometric studies

Flow cytometric analyses were performed on a Becton Dickinson FACScalibur instrument equipped with a 15 mW, 488 nm, air-cooled argon laser; data were analyzed using Cell Quest software (Becton Dickinson). The induction of apoptotic cell death and the effect on cell cycle distribution by the PSs were evaluated following 24 h exposure to the drugs at their respective IC_{50} values, 2 h irradiation in drug-free PBS and 24 h incubation in drug-free medium. To assess the percentage of apoptotic cells, the Annexin V-FITC apoptosis detection kit (BD, Pharmingen) was used according to the manufacturer's instructions. Briefly, cells were detached with trypsin/EDTA, washed in PBS and resuspended (1×10^6 cells/ml) in 1× binding buffer; 5 μl of Annexin V-FITC were added to 100 μl of each sample. Cells were incubated for 15 min in the dark, diluted with 400 μl of binding buffer and the percentage of apoptotic cells in each sample was evaluated based on the intensity of FITC-related fluorescence. To determine cell cycle distribution, cells were detached by trypsinization, washed in PBS and fixed in ice-cold 70% ethanol for 20 min at −20 °C. After a further wash in PBS, DNA was stained with 50 μg/ml propidium iodide in PBS in the presence of RNAse A (30 U/ml) at 37 °C for 30 min before analysis of the samples.

Intracellular generation of oxidizing species was determined using the fluorogenic probe 2′,7′-dichlorodihydrofluorescein diacetate (DCHF-DA, InVitrogen Molecular Probes). The diacetate moieties are cleaved by intracellular esterases to release the corresponding dichlorodihydrofluorescein derivative (non-fluorescent), that is readily oxidized to dichlorofluorescein (DCF) by reactive oxygen species (ROS). Cells were treated with PSs at their respective IC_{50} values for 24 h, followed by 2 h irradiation in drug-free PBS. Cells were detached at the end of the irradiation period, washed and resuspended (1×10^6 cells/ml) in PBS containing 5 μM DCFH-DA; cell samples were analyzed after 1 h incubation in the dark at 37 °C, and the amount of intracellular ROS generation is reported in arbitrary units based on the mean fluorescence intensity (MFI).

4.9. NO· generation

Nitrite accumulation, an indicator of NO· production, was measured over a period of 24 h in supernatants from HCT116 cells (exposed to the PSs at their respective IC_{50} values and irradiated as previously described) by a colorimetric assay based on the Griess reaction.[35] Briefly, cell supernatants were sampled at the end of the irradiation period and 24 h thereafter and reacted with equal volumes of Griess reagent (1% sulfanylamide and 0.1% naphtylethylenediamine dihydrochloride in 2.5% H_3PO_4) at room temperature for 10 min. NO_2^- concentration was determined based on the absorbance at 550 nm and referred to sodium nitrite standards. To assess the role of NO· generation in the photodynamic activity of compound **2**, HCT116 cells were co-incubated for 24 h with the NO·-synthase (NOS) inhibitor NG-monomethyl-L-arginine (L-NMMA) at the concentration of 1 mM together with the different concentrations of compound **2**, irradiated and processed for the MTT assay 24 h after the end of the irradiation period, as described above.

4.10. Statistical analysis

The effects of the three diarylporphyrins on HCT116 cells were compared with those of *m*-THPC by one-way analysis of variance; multiple comparisons were performed using Bonferroni post-test. The IC_{50} values of *m*-THPC and compound **4** were compared by means of Student's *t* test.

Acknowledgment

Partially supported by the Italian Ministry of University and Research, PRIN 2005.

References and notes

1. Brown, A. S.; Brown, E. A.; Walker, I. *Lancet Oncol.* **2004**, *35*, 497.
2. Dougherty, T. J.; Gomer, C. J.; Henderson, B. W.; Jori, G.; Kessel, D.; Korbelik, M.; Moan, J.; Peng, Q. *J. Natl. Cancer Inst.* **1998**, *90*, 889.
3. Moor, A. C. *J. Photochem. Photobiol. B* **2000**, *57*, 1.
4. Oleinick, N. L.; Evans, H. H. *Radiat. Res.* **1998**, *150*, S146.
5. Marchal, S.; Fadloun, A.; Maugain, E.; D'Hallewin, M.-A.; Guillemin, F.; Bezdetnaya, L. *Biochem. Pharmacol.* **2005**, *69*, 1167.
6. Almeida, R. D.; Manadas, B. J.; Carvalho, A. P.; Duarte, C. B. *Biochim. Biophys. Acta* **2004**, *1704*, 59.
7. Wyld, L.; Reed, M. W.; Brown, N. J. *Br. J. Cancer* **2001**, *84*, 1384.
8. MacDonald, I. J.; Dougherty, T. J. *J. Porphyr. Phthalocyanines* **2001**, *5*, 105.
9. Kessel, D.; Vicente, M. G.; Reiners, J. J., Jr. *Lasers Surg. Med.* **2006**, *38*, 482.
10. Moan, J.; Peng, Q. *Anticancer Res.* **2003**, *23*, 3591.
11. Detty, M. R.; Gibson, S. L.; Wagner, S. J. *J. Med. Chem.* **2004**, *47*, 3897.
12. Hopper, C.; Kubler, A.; Lewis, H.; Tan, I. B.; Putnam, G. *Int. J. Cancer* **2004**, *111*, 138.
13. D'Cruz, A.; Robinson, M. H.; Biel, M. A. *Head Neck* **2004**, *26*, 232.
14. Bourré, L.; Simonneaux, G.; Ferrand, Y.; Thibaut, S.; Lajat, Y.; Patrice, T. *J. Photochem. Photobiol. B* **2003**, *69*, 179.
15. Banfi, S.; Caruso, E.; Buccafurni, L.; Murano, R.; Monti, E.; Gariboldi, M.; Papa, E.; Gramatica, P. *J. Med. Chem.* **2006**, *49*, 3293.
16. Leung, W. N.; Sun, X.; Mak, N. K.; Yow, C. M. *Photochem. Photobiol.* **2002**, *75*, 406.

17. Buytaert, E.; Callewaert, G.; Hendrickx, N.; Scorrano, L.; Hartmann, D.; Missiaen, L.; Vandenheede, J. R.; Heirman, I.; Grooten, J.; Agostinis, P. *FASEB J.* **2006**, *20*, 756.
18. Marchal, S.; Francois, A.; Dumas, D.; Guillemin, F.; Bezdetnaya, L. *Br. J. Cancer* **2007**, *96*, 944.
19. Teiten, M. H.; Marchal, S.; D'Hallewin, M. A.; Guillemin, F.; Bezdetnaya, L. *Photochem. Photobiol.* **2003**, *78*, 9.
20. Hsieh, Y. J.; Wu, C. C.; Chang, C. J.; Yu, J. S. *J. Cell. Physiol.* **2003**, *194*, 363.
21. Henderson, B. W.; Dougherty, T. J. *Photochem. Photobiol.* **1992**, *55*, 145.
22. Gilaberte, Y.; Pereboom, D.; Carapeto, F. J.; Alda, J. O. *Photodermatol. Photoimmunol. Photomed.* **1997**, *13*, 43.
23. Nyman, E. S.; Hynninen, P. H. *J. Photochem. Photobiol B* **2004**, *73*, 1.
24. Moncada, S. R.; Palmer, R. M. J.; Higgs, E. A. *Pharmacol. Rev.* **1991**, *43*, 109.
25. Hempel, S. L.; Buettner, G. R.; O'Malley, Y. Q.; Wessels, D. A.; Flaherty, D. M. *Free Radic. Biol. Med.* **1999**, *27*, 146.
26. Gupta, S.; Ahmad, N.; Mukhtar, H. *Cancer Res.* **1998**, *58*, 1785.
27. Ali, S. M.; Olivo, M. *Int. J. Oncol.* **2003**, *22*, 751.
28. Yamamoto, F.; Ohgari, Y.; Yamaki, N.; Kitajima, S.; Shimokawa, O.; Matsui, H.; Taketani, S. *Biochem. Biophys. Res. Commun.* **2007**, *353*, 541.
29. Gomes, E. R.; Almeida, R. D.; Carvalho, A. P.; Duarte, C. B. *Photochem. Photobiol.* **2002**, *76*, 423.
30. Niziolek, M.; Korytowski, W.; Girotti, A. W. *Free Radic. Biol. Med.* **2006**, *40*, 1323.
31. Niziolek, M.; Korytowski, W.; Girotti, A. W. *Free Radic. Biol. Med.* **2003**, *34*, 997.
32. Niziolek, M.; Korytowski, W.; Girotti, A. W. *Photochem. Photobiol.* **2003**, *78*, 262.
33. Alley, M. C.; Scudiero, D. A.; Monks, A.; Hursey, M. L.; Czerwinski, M. J.; Fine, D. L.; Abbott, B. J.; Mayo, J. G.; Shoemaker, R. H.; Boyd, M. R. *Cancer Res.* **1988**, *48*, 589.
34. Katona, Z.; Grofcsik, A.; Baranyai, P.; Bitter, I.; Grabner, G.; Kubinyi, M.; Vidóczy, T. *J. Mol. Struct.* **1998**, *450*, 41.
35. Green, L. C.; Wagner, D. A.; Glogowski, J.; Skipper, P. L.; Wishnok, J. S.; Tannenbaum, S. R. *Anal. Biochem.* **1982**, *126*, 131.